The Monte Carlo Simulation of Radiation Transport

Alex F Bielajew
The University of Michigan
Department of Nuclear Engineering and Radiological Sciences
2927 Cooley Building
2355 Bonisteel Boulevard
Ann Arbor, Michigan 48109-2104
U. S. A.
Tel: 734 764 6364
Fax: 734 763 4540
email: bielajew@umich.edu

August 1, 2001

Introduction

As applied to radiation transport applications in radiotherapy and dosimetry, the Monte Carlo method provides a numerical solution to the Boltzmann transport equation that employs directly the fundamental microscopic physical laws of electron-atom and photon-atom interactions. The fluences of individual particle tracks are faithfully reproduced within our knowledge of the physical laws—the scattering and absorption cross sections. Macroscopic features of the radiation fields, for example the average track-length per incident photon in a given volume of space, is computed as an average over many individual particle simulations. If the true average $\overline{x}$ exists and the distribution in x has a true finite variance, σ_x^2, the *Central Limit Theorem* (Lindeberg 1922; Feller 1967) *guarantees* that the Monte Carlo *estimator* for $\overline{x}$, that we shall call $\langle x \rangle$, can be made arbitrarily close to $\overline{x}$ by increasing the number, N, of particle *histories* simulated. Moreover, the Central Limit Theorem predicts that the dis-

tribution of $\langle x \rangle$ is Gaussian characterized by a variance $\sigma^2_{\langle x \rangle}$ that may be estimated simply in the simulation. The Central Limit Theorem also predicts that in the limit $N \longrightarrow \infty$, $\sigma^2_{\langle x \rangle} \longrightarrow 0$. This limiting result is also proven by the *Strong Law of Large Numbers* (Feller 1967).

These are very powerful and compelling facts, which have been partly responsible for the geometric increase in the use of the Monte Carlo method in radiotherapy and dosimetry applications (Nahum 1989), a trend that has continued since Nahum's review article. If one knows the governing physical laws to sufficient accuracy and has access to sufficient computing resources, then the answer to any well-posed physical question may be computed. Fortunately, the physical laws required for most applications in radiotherapy and dosimetry are well known. They are the results of Quantum Electrodynamics (QED) (Bjorken and Drell 1964; Bjorken and Drell 1965; Sakurai 1967), one of the most successful theories of Theoretical Physics. Additionally, the computer resources required for most of our applications are modest and may be executed to sufficient accuracy on run-of-the-mill desktop computers and workstations. At the time when this article is being written, this confluence of theory and computational ability is putting the Monte Carlo method into the standard toolbox of the research medical physicist.

There are, of course, significant technical obstacles to be overcome. However, these obstacles are surmountable. The point of this article is to demonstrate the power and utility of the Monte Carlo method without the necessary detail that would be considered in a much more lengthy article. Fortunately, there are some excellent detailed reviews on this topic (Rogers and Bielajew 1990; Mackie 1990; Andreo 1991). The reader should bear in mind that an application with tens of thousands of volume elements and many different materials to describe a simulation geometry is only slightly more complicated than a simple two-medium interface problem. More organization and computer coding is required, but the technical ability to solve the simpler problem empowers one with the ability to solve the more complex problem.

A brief history of Monte Carlo

Usually, the first reference to the Monte Carlo method is that of Comte de Buffon (1777) who proposed a Monte Carlo-like method to evaluate the probability of tossing a needle onto a ruled sheet. This reference goes back to 1777, well before the contemplation of automatic calculating machines. Buffon calculated that a needle of length L tossed randomly on a plane ruled with parallel lines of distance d apart where $d > L$ would have a probability

$$p = \frac{2L}{\pi d} \ . \tag{1}$$

A computer simulation of 50 needles (where $d/L = \frac{3}{4}$) on a finite grid of 5 lines is shown in Figure 1.

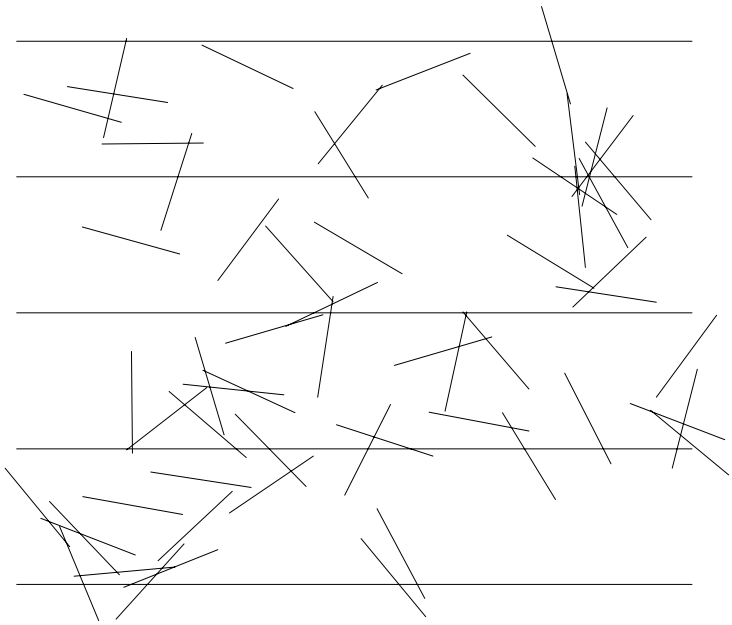

Figure 1: A computer simulation of the Buffon needle problem.

Much later, Laplace (1886) suggested that this procedure could be employed to determine the value of π, albeit slowly. Several other historical uses of Monte Carlo predating computers are cited by Kalos and Whitlock (1986). The modern Monte Carlo age was ushered in by von Neumann and Ulam during the initial development of thermonuclear weapons[1]. Ulam and von Neumann coined the phrase "Monte Carlo" and were pioneers in the development of the Monte Carlo technique and its realizations on digital computers[2].

[1]The two books by Richard Rhodes, *The making of the Atomic Bomb* and *Dark Sun* are excellent historical sources for this period.

[2]Despite their chequered history, thermonuclear weapons have never been deployed in conflict. So Monte Carlo calculations have not been employed in a destructive way. In contrast, Monte Carlo calculations are employed for beneficial purposes, such as in the prediction of dose in cancer treatments (Bielajew 1994) and should be credited with saving lives.

Photon interaction processes

The photon interaction processes that should be modeled by a Monte Carlo code designed for applications in radiotherapy and dosimetry are:

- Pair production in the nuclear and atomic fields (Davies, Bethe, and Maximon 1954; Motz, Olsen, and Koch 1969; Tsai 1974)
- Compton scattering from atomic electrons (incoherent scattering) (Klein and Nishina 1929; Compton and Allison 1935)
- Photoelectric absorption and photoelectron production (Sauter 1931)
- Rayleigh scattering from atomic and molecular fields (coherent scattering) (Rayleigh 1871)

These processes are reviewed in systematic detail by Evans (1955) and in somewhat more approachable manner by others (Johns and Cunningham 1983; Attix 1986; Shultis and Faw 1996). Tables of photon cross sections are tabulated by Hubbell and Øverbø (1979).

We now consider the relative importance of the various processes involved for materials common to radiotherapy applications. For water and bone, the relative strengths of the photon interactions versus energy are shown in Figure 2, along with the *mean free path,* the average distance a photon travels before interacting via one of the interaction processes just discussed. For these materials we note three distinct regions of single interaction dominance: photoelectric below 20 keV, pair above 30 MeV and Compton in between. The Rayleigh interaction is about an order of magnitude smaller. Note that the material composition of water and bone is quite different. Water is a molecule with molecular composition H_2O and density of 1.00 g/cm^3. The bone composition employed in the creation of Figure 2 was (H:0.034|C:0.155|N:0.042|O:0.435|Na:0.001|Mg:0.002|P:0.103|S:0.003000|Ca:0.225) by weight fractions with a density of 1.92 g/cm^3. Figure 2(a) shows a subtle narrowing of bone's Compton dominant region, with somewhat more photoelectric and pair contributions from bone's higher-Z components. When the mean free path is presented in units of g/cm^2, we see that the mean free path in bone is almost the same between 100 keV and 10 MeV and higher outside of this range. These differences may be modeled quite easily with Monte Carlo methods.

We also note from Figure 2(b) that the interaction distances of photons in the energy range 10 keV $\leq E_\gamma \leq$ 40 MeV is O(cm) for common low-Z materials. This means that if one considers the transport of γ's alone, it is feasible, with modest computational resources, to simulate many millions of particle histories. This is because the γ's will interact only a few times in macroscopic objects, such as a radiation measuring device, a tank of water, or a human being being treated with radiotherapy[3].

[3]Monte Carlo based treatment planning requires of the order of 10^8–10^9 photon histories.

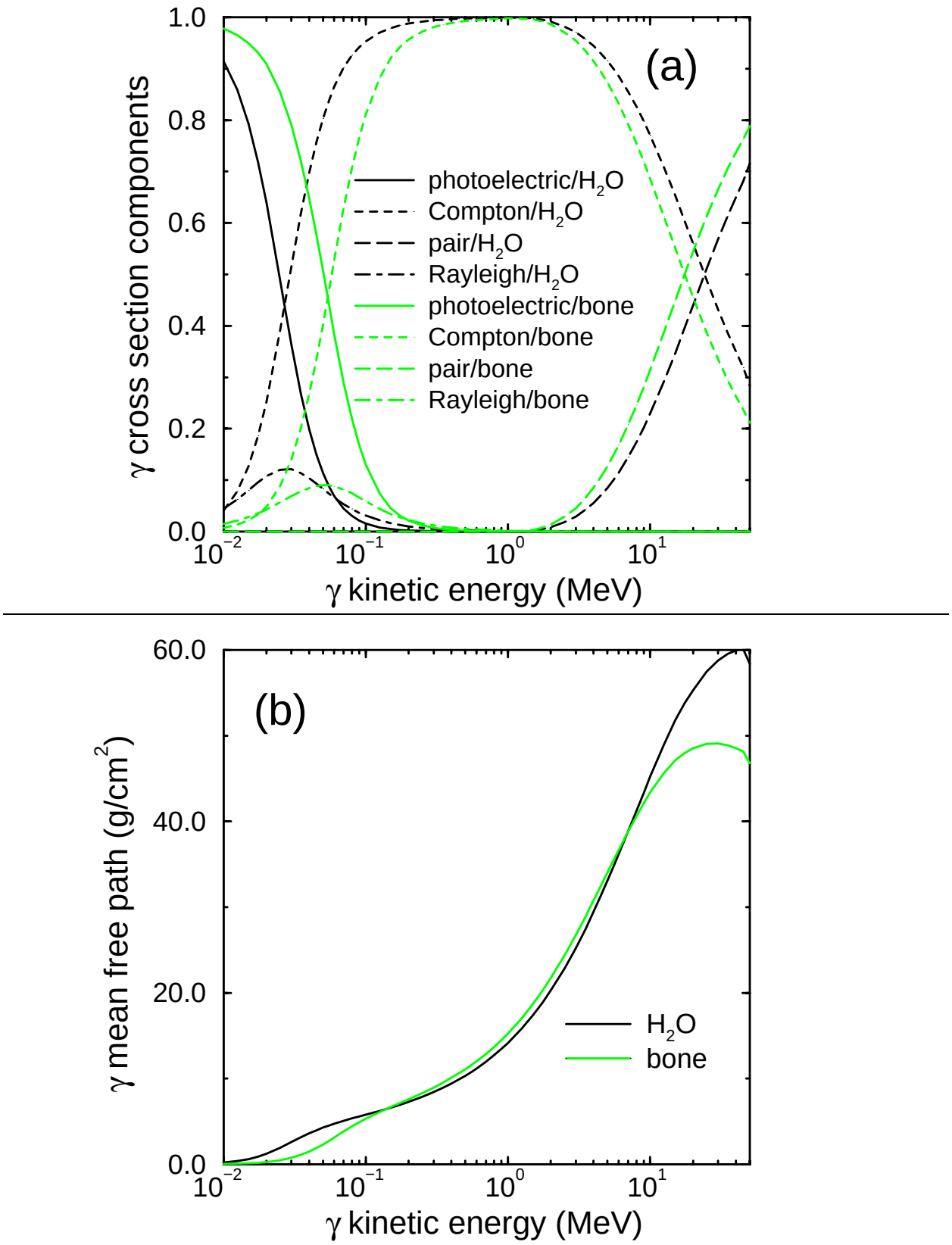

Figure 2: **(a)** Components of the photon cross section in water and bone, **(b)** Mean free path of photons in water and bone. [Data extracted from the EGS4 code system (Nelson, Hirayama, and Rogers 1985).]

Electron interaction processes

The electron and positron interaction processes that should be modeled by a Monte Carlo code designed for applications in radiotherapy and dosimetry are:

- Møller scattering of electrons from atomic electrons (Møller 1932),
- Bhabha scattering of positrons from atomic electrons (Bhabha 1935),
- Bremsstrahlung photon creation in the nuclear and atomic fields (Koch and Motz 1959; Tsai 1974),
- Positron annihilation with atomic electrons (Heitler 1954),
- Elastic scattering of electrons and positrons from nuclei (Mayol and Salvat 1997),
- Excitation of atoms and molecules by electrons and positrons.

Figure 3 presents the electron mean free paths for the elastic, ionization, excitation and bremsstrahlung interactions in oxygen. We note that the distance to an interaction in the relativistic region (greater than, say, 1 MeV) is in the 10^{-5}–10^{-4} g/cm^2. The range of a 10 MeV electron in oxygen is 5.6 g/cm^2. This means, for example, that a relativistic electron must undergo 10^5–10^6 interactions before slowing down. A typical electron is completely slowed down in a typical simulation geometry. This means that each one of the 10^5–10^6 interactions would have to be simulated for *each* electron history! This form of calculation is called *analog* simulation and requires Teraflop computational resources for most practical problems.

Fortunately, there is a practical solution to this problem, first pioneered by Berger (Berger 1963). Berger called his technique *Condensed History Electron Transport.* It is based on the realization that while electrons undergo many interactions, relatively few of these interactions cause a great deal of energy loss or directional change. The effect of most of these interaction is small, involving little energy loss or small angular deflections. Therefore, one can *combine* the effect of these small-effect interactions into single virtual large-effect interactions. These large-effect interactions can be predicted theoretically through cumulative-event theories. For energy losses, there is the continuous slowing down (CSD) method with the energy loss being characterized by the stopping power (Bethe 1930; Bethe 1932; Bloch 1933) or by distributions that are a function of the length of the electron path (Landau 1944; Vavilov 1957). The effect of cumulative elastic scattering events are predicted by several "small-angle" theories (Bothe 1921b; Bothe 1921a; Wentzel 1922; Eyges 1948; Molière 1947; Molière 1948; Bethe 1953) although these are now losing favor to the "any-angle" theory of Goudsmit and Saunderson (1940a, 1940b). All of these theories require single-event elastic scattering models. The Goudsmit–Saunderson approach is favored because it can be employed to use any cross section. In particular, elastic cross section calculations using partial-wave analysis are becoming quite sophisticated (Salvat and Mayol 1993a; Salvat and Mayol 1993b; Mayol and Salvat 1997) and are being adopted in advanced Monte Carlo algorithms. Fortunately, the elastic scattering that produces the angular deflections produces no energy loss and is not strongly dependent on energy. Additionally, the energy-loss process produces very little

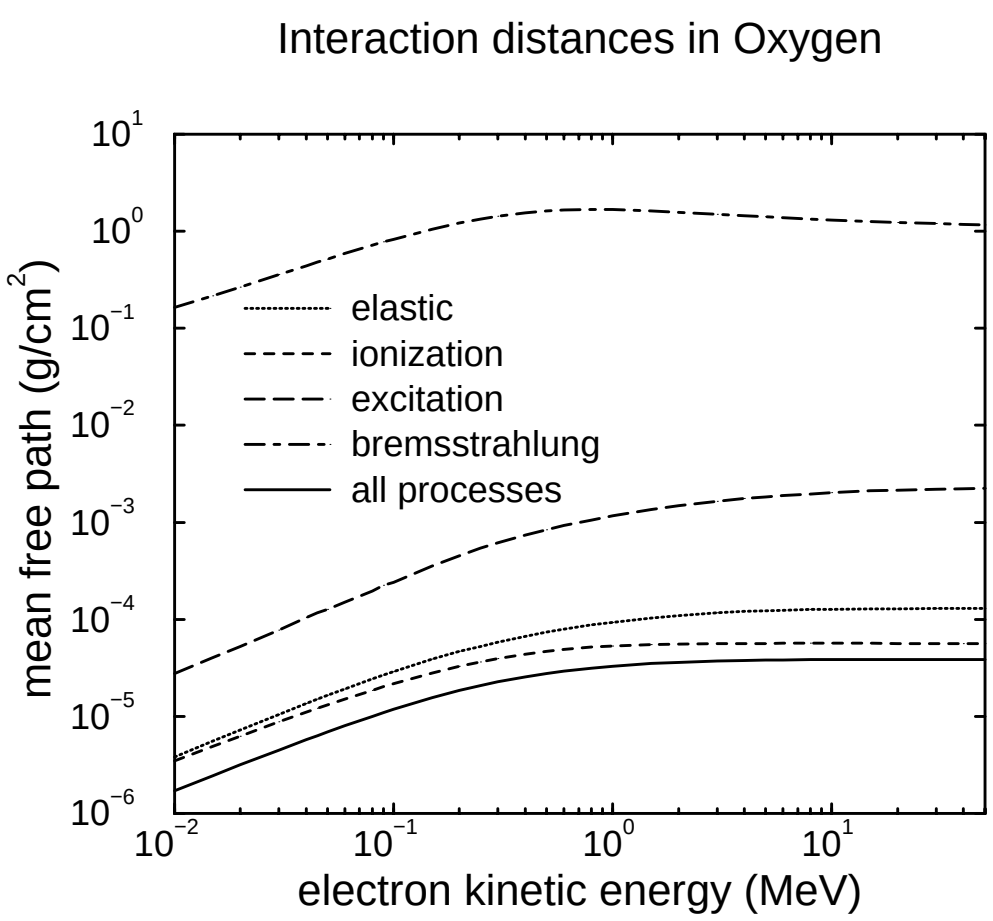

Figure 3: Electron elastic, ionization, excitation and bremsstrahlung cross sections in Oxygen. [Data derived from the Lawrence Livermore Evaluated Electron Data Library (Perkins, Cullen, and Seltzer 1991).]

angular deflection. Therefore, these two process nearly decouple, making the theoretical development somewhat simplified and the construction of algorithms somewhat easier. (High accuracy approaches have to consider this coupling and treat it carefully (Kawrakow and Bielajew 1998b; Kawrakow and Bielajew 1998a).

Recently, the Condensed History Method (CHM) has been put on a stronger theoretical footing by Larsen (Larsen 1992), who showed that CHM converges to the exact solution of the Boltzmann transport equation in the limit the electron pathlengths are made small. This is actually a warning that the CHM is an *approximation* and its use can lead to calculational artefacts when applied outside of its range of validity (Bielajew, Rogers, and Nahum 1985; Bielajew and Rogers 1989; Seltzer 1991). This has led to the development of high-accuracy CHM's (Bielajew and Rogers 1987; Seltzer 1991; Fernández-Varea, Mayol, Baró, and Salvat 1993; Kawrakow and Bielajew 1998a). Research in this area remains quite active.

The benefits of adopting the CHM is evident in the "partial" mean free paths depicted in Figure 4.

In this figure the mean free path to a bremsstrahlung interaction and a Møller interaction (δ-creation event) are shown for secondary particle thresholds of 1, 10 and 100 keV. The analog Monte Carlo method is employed for interactions that produce secondary particles above the thresholds. The CSD or other energy-loss methods are employed for the sub-threshold events. We note that higher thresholds produce longer mean free paths and more efficient calculation. This is traded for a loss of information on particle fluences below the thresholds. These thresholds become important parameters that a Monte Carlo practitioner must select depending on the application. Selection of these thresholds (and other parameters like electron pathlength) becomes one of the "skills" of the Monte Carlo user. Further information on these parameters is best obtain from the extensive literature describing the various general-purpose Monte Carlo codes available, such as EGS4 (Nelson, Hirayama, and Rogers 1985; Bielajew, Hirayama, Nelson, and Rogers 1994), ETRAN (Seltzer 1989; Seltzer 1991), ITS (Halbleib and Mehlhorn 1984; Halbleib 1989; Halbleib, Kensek, Mehlhorn, Valdez, Seltzer, and Berger 1992), MCNP (Briesmeister 1986; Briesmeister 1993; Briesmeister 1997), and PENELOPE (Baró, Sempau, Fernández-Varea, and Salvat 1995; Salvat, Fernández-Varea, Baró, and Sempau 1996; Sempau, Acosta, Baró, Fernández-Varea, and Salvat 1997).

Coupled electron-photon transport

The process by which coupled electron-photon transport is carried out is described in Figure 5.

In Figure 5(a) the simulation geometry is depicted by the outer rectangular box. Photons are represented by straight dashed lines, electrons and positrons by solid curves. A photon starts the simulation by insertion, **I**, into the simulation geometry. It undergoes a pair interaction **P** producing an e^-e^+ pair. The electron track (on the left) undergoes a bremsstrahlung interaction at **B**. Following the photon we see that there is a Compton interaction at **C**. The resulting electron is then transported until it runs out of energy at **X**. The photon undergoes a Rayleigh interaction at **R** and is then absorbed in a photoelectric event at **Ph**. The photoelectron escapes the simulation geometry at **E**. Returning to the initial electron, it undergoes a Møller interaction at **M**. Both the electron and its knock-on are then transported until their end-of range at the **X**'s. The positron that was born in the pair interaction at **P** undergoes a bremsstrahlung interaction at **B**, followed by a Bhabha interaction at **Bh**. The electron from **B** reaches its end-of-range at **X**. The positron eventually annihilates, producing two back-to-back annihilation quanta that escape the simulation geometry at their respective **E**'s. We now focus in on the details of the CHM depicted in Figure 5(b). At each one of the vertices, represented by a solid circle, the positron changes direction. (Electron and positron transport in the CHM are essentially the same.) The deposition of energy according to the CSD or other models can be considered to happen anywhere along the track segments.

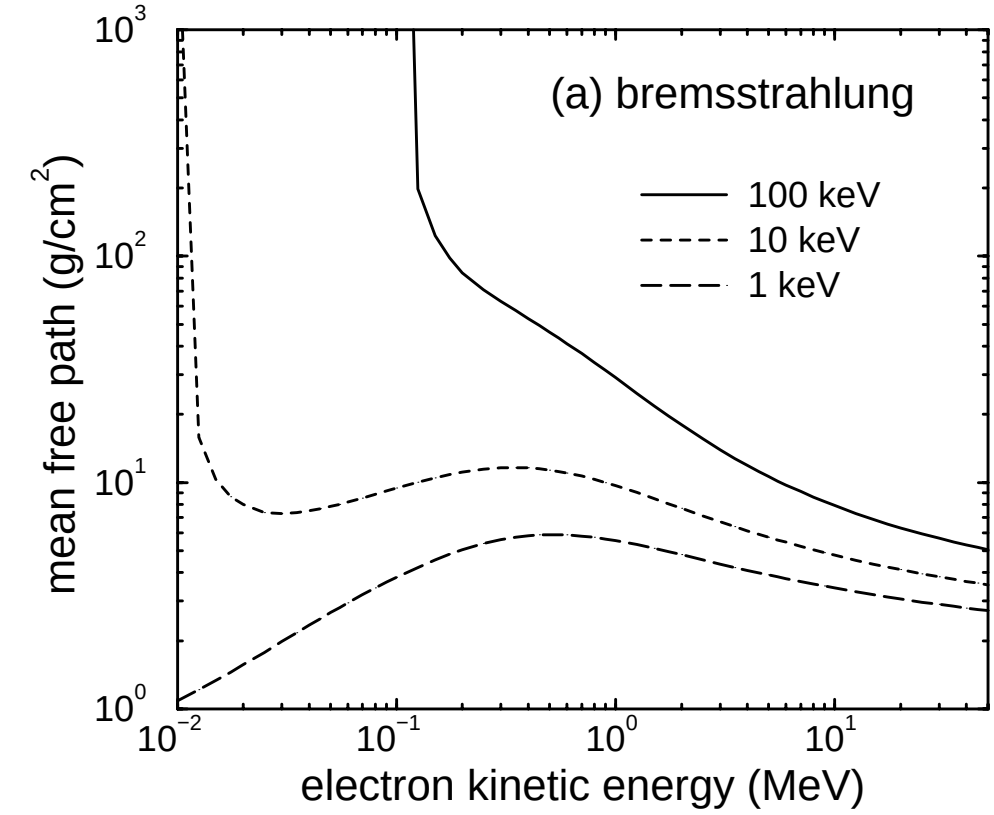

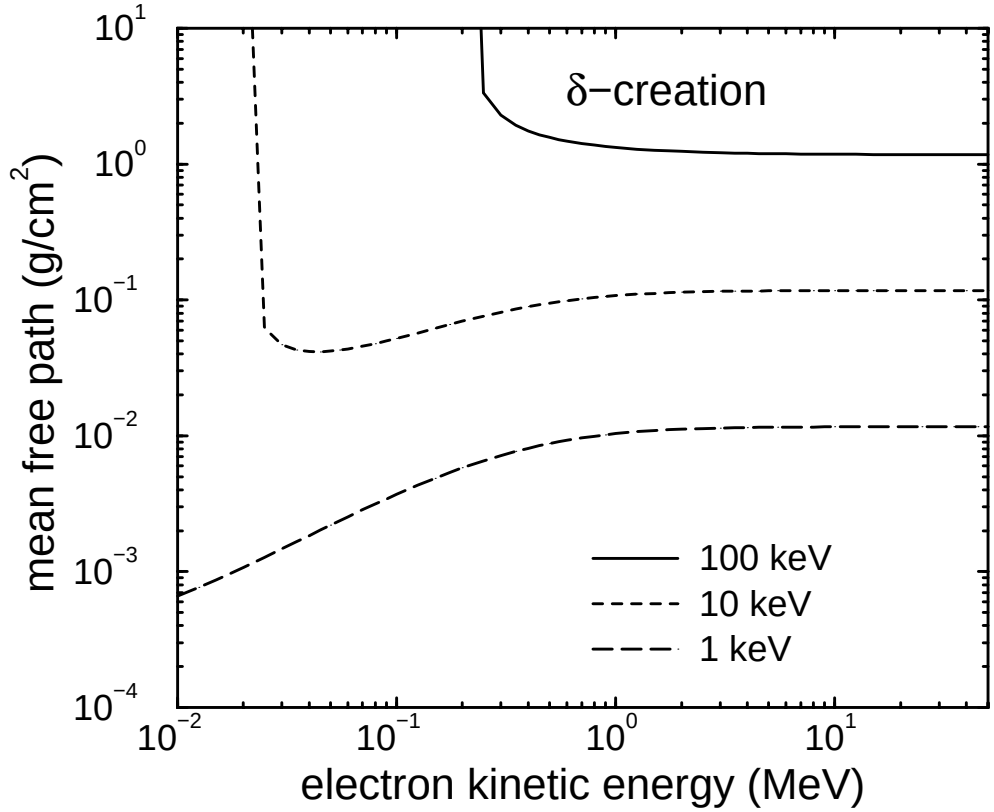

Figure 4: Mean free path to a bremsstrahlung interaction **(a)** or a Møller interaction **(b)** for different thresholds (Data extracted from the EGS4 code system (Nelson, Hirayama, and Rogers 1985).)

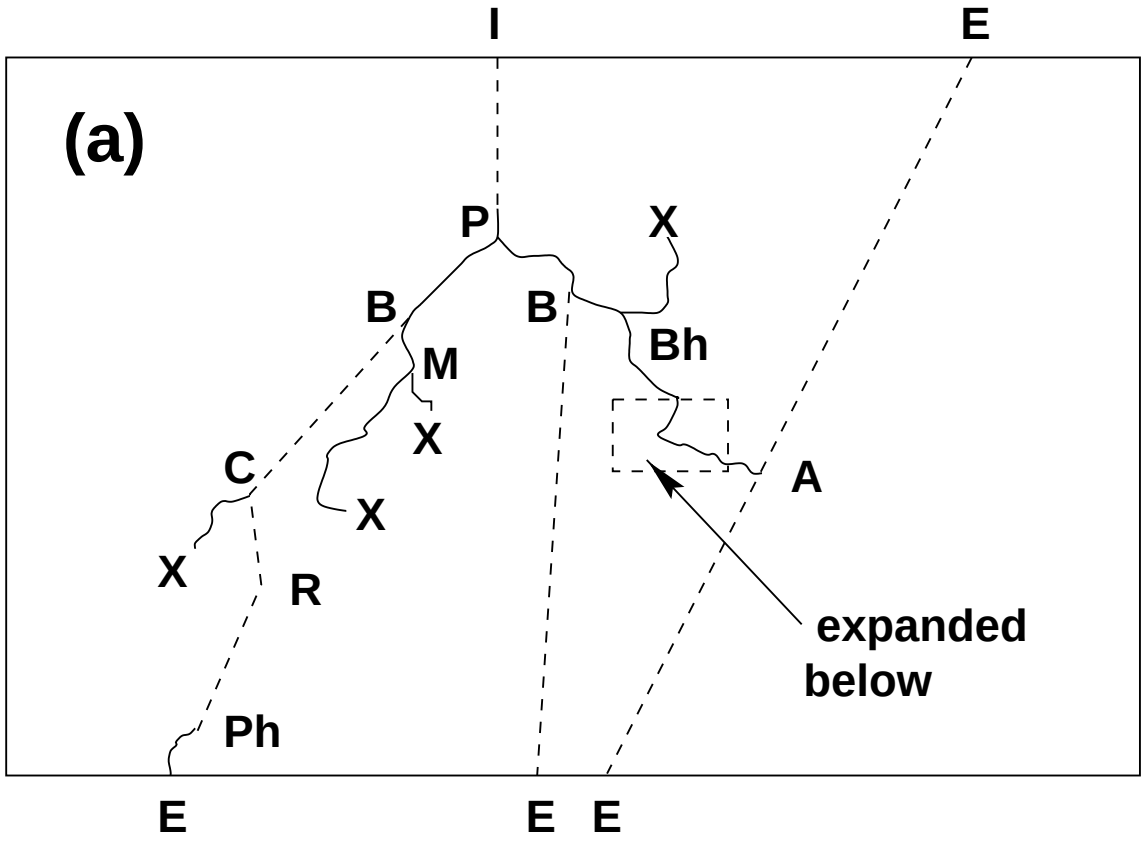

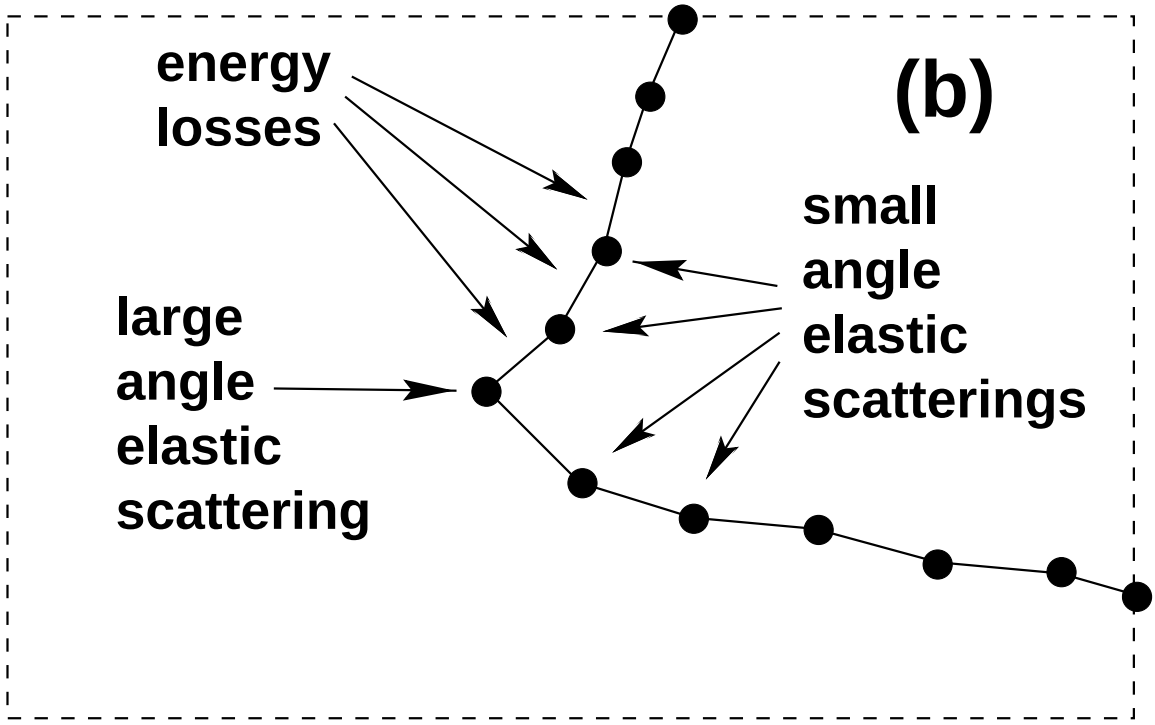

Figure 5: **(a)** Global picture of electron transport. Photons are represented by straight dashed lines, electrons and positrons by solid curves. (I:Insertion, E:Escape, P:Pair production, B:Bremsstrahlung, M:Møller X:End-of-range, C:Compton, R:Rayleigh, Ph:Photoelectric, Bh:Bhabha, A:Annihilation) **(b)** Expanded version of the dashed box in **(a)**

Mathematical methods of Monte Carlo

Before concluding this chapter, we will discuss some of the basic mathematics of the Monte Carlo method. A complete discussion would involve a discussion of random number generation (RNG), sampling theory, displacements and rotations, estimating means and variances, and geometry. With insufficient space remaining, we will reference most of the requisite material.

Random Number Generation

We shall assume that we have a good source of random numbers. Much mathematical study has been devoted to RNG (Ehrman 1981; Knuth 1981; James 1988). These three references are excellent reviews of RNG theory and methods up to about 1987. The following references contain more modern material (Marsaglia, Zaman, and Tsang 1990; Marsaglia and Zaman 1991; Lüscher 1994; James 1994; Knuth 1997). It must also be noted that random number generation is an area of active research. Information that was given last year may be proven to be misleading this year. The best way to stay in tune is to track the discussions concerning this topic on the web sites of organizations for which random number generation is critical. A particularly good site is CERN's site (www.cern.ch). CERN is the European Laboratory for Particle Physics. Monte Carlo applications are quite important in particle physics.

Elementary Sampling Theory

Assume that we have a probability function $p(x)$ that is normalized over some range between a and b, that is,

$$\int_a^b \mathrm{d}x' \; p(x') = 1 \; . \tag{2}$$

We now construct its cumulative probability distribution function:

$$c(x) = \int_a^x \mathrm{d}x' \; p(x') \; , \tag{3}$$

that is nondecreasing and bounded between 0 and 1. It can be shown that a variable x is distributed randomly according to $p(x)$ if we select x's according to the inverse of $c(x)$ according to

$$x = c^{-1}(\xi) \; , \tag{4}$$

where ξ is a uniformly distributed random number between 0 and 1.

For example, it can be shown that the distance to an interaction can be sampled from:

$$x = -\Sigma^{-1} \log(1 - \xi) \; , \tag{5}$$

where Σ^{-1} is the macroscopic cross section. This follows directly from the probability distribution for interaction distances,

$$p(x) = \Sigma \exp(-\Sigma x) \quad 0 \leq x \leq \infty \ . \tag{6}$$

We note that the function inversion technique implicit in Equation 4 may not always be possible analytically, but it is *always* possible numerically! Other sampling techniques are discussed elsewhere (Nelson, Hirayama, and Rogers 1985; Bielajew 1993).

Displacements and rotations

Ray tracing (displacement and rotation) is carried out using very simple geometrical constructs. Given that a particle has a position $\vec{x}_0$ and direction $\vec{u}_0$ and distance to travel s, the new position, $\vec{x}$, is given by:

$$\vec{x} = \vec{x}_0 + \vec{u}_0 s, \tag{7}$$

where $\vec{u}_0 = (u_0, v_0, w_0) = (\sin\theta_0 \cos\phi_0, \sin\theta_0 \sin\phi_0, \cos\theta_0)$, θ_0 and ϕ_0 are the polar and azimuthal angles respectively.

Rotation after a scattering by polar angle Θ and azimuthal angle Φ is carried out via the rotation:

$$\begin{aligned} u = \sin\theta\cos\phi &= u_0 \cos\Theta + \sin\Theta(w_0 \cos\Phi \cos\phi_0 - \sin\Phi \sin\phi_0) \ , \\ v = \sin\theta\sin\phi &= v_0 \cos\Theta + \sin\Theta(w_0 \cos\Phi \sin\phi_0 + \sin\Phi \cos\phi_0) \ , \\ w = \cos\theta &= w_0 \cos\Theta - \sin\Theta \sin\theta_0 \cos\Phi \ , \end{aligned} \tag{8}$$

that provides the new direction for the particle after a scattering.

Estimating means and variances

The conventional approach to calculating the estimated error is as follows:

- Assume that the calculation calls for the simulation of N particle histories.
- Assign and accumulate the value x_i for the score associated with the i'th history, where $1 \leq i \leq N$. Assign as well the square of the score x_i^2 for the i'th history.
- Estimate the mean value of x:

$$\langle x \rangle = \frac{1}{N} \sum_{i=1}^{N} x_i \tag{9}$$

- Estimate the variance associated with the distribution of the x_i:

$$s_x^2 = \frac{1}{N-1}\sum_{i=1}^{n}(x_i - \langle x\rangle)^2 = \frac{1}{N-1}\sum_{i=1}^{n}(x_i^2 - \langle x\rangle^2) \tag{10}$$

- The estimated variance of $\langle x\rangle$ is the standard variance of the mean:

$$s_{\langle x\rangle}^2 = \frac{s_x^2}{N} \tag{11}$$

  Note that it is the error in $\langle x\rangle$ we are seeking, not the "spread" of the distribution of the x_i.

- Report the final result as $\langle x\rangle = \pm s_{\langle x\rangle}$.

  The Central limit Theorem interpretation is that $\langle x\rangle$ satisfies $|\overline{x} - \langle x\rangle| < s_{\langle x\rangle}$ 68% of the time.

Geometry

Geometrical elements are made up of regions of space bounded by planes and quadric surfaces (spheres, cylinders, *etc*). The essential problem is to determine the smallest intercept distance along the forward flight direction to one of the bounding surfaces. A well-defined prescription for doing this (Nelson and Jenkins 1987; Bielajew 1995) is summarized below.

Borrowing from the notation of Olmsted (1947), an arbitrary quadric surface in 3(x,y,z)-space[4] can be represented by:

$$f(\vec{x}) = \sum_{i,j=0}^{3} a_{ij}x_i x_j = 0. \tag{12}$$

The a_{ij}'s are arbitrary constants and the 4-vector x_i has components $(1, x, y, z)$. The zeroth component is unity by definition ,allowing a very compact representation and a_{ij} is symmetric with respect to the interchange of i and j, that is $a_{ij} = a_{ji}$. Equation 12 is very general and encompasses a wide variety of possibilities, including solitary planes (*e.g.* only a_{0i} non-zero), intersecting planes (*e.g.* only a_{11} and a_{22} non-zero), cylinders (circular, elliptical, parabolic and hyperbolic), spheres, spheroids and ellipsoids, cones (circular and elliptical), hyperboloids of one and two sheets and elliptic and hyperbolic paraboloids. These surfaces can be combined to make geometrical objects of great complexity and are extremely useful in Monte Carlo modeling of physical objects.

Despite having apparently 10 independent constants, Equation 12 represents only 10 independent real surfaces (including the simple plane), unique after a translation and rotation

[4]The only variance with Olmsted's notation is that the 4^{th} component is labelled as the 0^{th} component in this work.

to standard position. The three cross terms (a_{ij} for $i \neq j$ and $i, j \geq 1$) can be eliminated by rotation. The resultant equation then only involves terms like x_i^2 and x_i. In addition, providing that a given variable's quadratic constant is non-zero, the linear terms can be eliminated by a translation. The result is that there are only two generic forms:

$$f(\vec{x}) = \sum_{i=1}^{3} a_i x_i^2 + c = 0, \tag{13}$$

and

$$f(\vec{x}) = \sum_{i=1}^{2} a_i x_i^2 + b x_3 = 0. \tag{14}$$

Equations 13 and 14 describe only 10 distinct possibilities with real solutions.

1. **ellipsoids:** $a_1^2 x_1^2 + a_2^2 x_2^2 + a_3^2 x_3^2 - c^2 = 0.$
2. **cones:** $a_1^2 x_1^2 + a_2^2 x_2^2 - a_3^2 x_3^2 = 0.$
3. **cylinders:** $a_1^2 x_1^2 + a_2^2 x_2^2 - c^2 = 0.$
4. **hyperboloids of one sheet:** $a_1^2 x_1^2 + a_2^2 x_2^2 - a_3^2 x_3^2 - c^2 = 0.$
5. **hyperboloids of two sheets:** $a_1^2 x_1^2 + a_2^2 x_2^2 - a_3^2 x_3^2 + c^2 = 0.$
6. **elliptic paraboloids:** $a_1^2 x_1^2 + a_2^2 x_2^2 + a_3 x_3 = 0.$
7. **hyperbolic paraboloids:** $a_1^2 x_1^2 - a_2^2 x_2^2 + a_3 x_3 = 0.$
8. **hyperbolic cylinders:** $a_1^2 x_1^2 - a_2^2 x_2^2 + c^2 = 0.$
9. **parabolic cylinders:** $a_1^2 x_1^2 + a_3 x_3 = 0.$
10. **simple planes:** $a_3 x_3 + c = 0.$

There are other imaginary surfaces (*e.g.* imaginary ellipsoids $a_1^2 x_1^2 + a_2^2 x_2^2 + a_3^2 x_3^2 + c^2 = 0$) that we will not consider, nor will we consider quadrics that can be made up of two independent planes in various orientations (*e.g.* intersection planes $a_1^2 x_1^2 - a_2^2 x_2^2 = 0$, parallel planes $a_1^2 x_1^2 - c^2 = 0$, and coincident planes $a_1^2 x_1^2 = 0$).

For more information on the reduction to canonical form, the reader is encouraged to read Olmsted's book (1947). Olmsted also gives the classification of the surfaces and lists the entire set of 17 canonical quadric forms.

To calculate the intercept distance to an arbitrary quadric surface, consider that the particle's trajectory is given by:

$$\vec{x} = \vec{p} + \vec{\mu} s \ , \tag{15}$$

where the starting position of the particle is $\vec{p} = (p_x, p_y, p_z)$. A positive value of s expresses a distance along the direction that the particle is going (forward trajectory) and a negative value is associated with a distance that the particle came from (backward trajectory). Thus, negative solutions that are found for s below will be rejected.

In Monte Carlo particle transport calculations as well as ray-tracing algorithms, a common problem is to find the distance a particle has to travel in order to intersect a surface. This is done by substituting for $\vec{x}$ from Equation 15 in Equation 12 to give:

$$s^2 \left(\sum_{i,j=0}^{3} a_{ij} \mu_i \mu_j \right) + 2s \left(\sum_{i,j=0}^{3} a_{ij} p_i \mu_j \right) + \left(\sum_{i,j=0}^{3} a_{ij} p_i p_j \right) = 0, \tag{16}$$

where we have adopted the convention that $\mu_0 = 0$ and $p_0 = 1$. This is a quadratic equation in s of the form $A(\vec{\mu})s^2 + 2B(\vec{\mu}, \vec{p})s + C(\vec{p}) = 0$ where $A(\vec{\mu}) = \sum_{i,j=0}^{3} a_{ij}\mu_i\mu_j$, $B(\vec{\mu}, \vec{p}) = \sum_{i,j=0}^{3} a_{ij} p_i \mu_j$ and $C(\vec{p}) = \sum_{i,j=0}^{3} a_{ij} p_i p_j$.

The intercept distance is given by the smallest positive solution of the above quadratic equation.

Conclusion

This chapter merely skims the surface of the Monte Carlo method as applied to radiotherapy and dosimetry. However, we can not overstate the simplicity of the approach and the powerful conclusions. With sufficient computational resources, we can answer any well-posed question as accurately as our knowledge of the basic cross sections allows us. Other approaches suffer from systematic uncertainties that may be impossible to estimate. However, these methods may be useful if the computational time for a Monte Carlo approach is prohibitive. The phrase *Don't be in a hurry to get the wrong answer!* is relevant in this respect[5]. If a computation is feasible by Monte Carlo methods, one is not required to estimate systematic errors, and one may proceed with some confidence to tackle other problems. If one factors in the human effort, ultimately the Monte Carlo approach may prove to be the most productive.

[5]According Dermott (Red) Cullen of Lawrence Livermore National Laboratory (LLNL), the originator of this expression, in reference to Monte Carlo calculations, was Bob Howerton (LLNL, *ca.* 1974) who said "Obviously, we are never in a rush for the wrong answer." However, Red Cullen's paraphrase "Don't be in a hurry to get the wrong answer!" seems somewhat preferable to this author.—AFB

References

Andreo P 1991 Monte Carlo techniques in medical radiation physics *Phys. Med. Biol.* **36** 861 – 920

Attix F H 1986 *Introduction to Radiological Physics and Radiation Dosimetry* New York: Wiley

Baró J, Sempau J, Fernández-Varea J M and Salvat F 1995 PENELOPE: An algorithm for Monte Carlo simulation of the penetration and energy loss of electrons and positrons in matter *Nuclear Instruments and Methods* **B100** 31 – 46

Berger M J 1963 Monte Carlo Calculation of the penetration and diffusion of fast charged particles *Methods in Comput. Phys.* **1** 135 – 215

Bethe H A 1930 Theory of passage of swift corpuscular rays through matter *Ann. Physik* **5** 325

Bethe H A 1932 Scattering of electrons *Z. für Physik* **76** 293

Bethe H A 1953 Molière's theory of multiple scattering *Phys. Rev.* **89** 1256 – 1266

Bhabha H J 1935 *Proc. Royal Society London* **A154** 195

Bielajew A F 1993 Efficiency, statistics and sampling *National Research Council of Canada Report PIRS-0395*

Bielajew A F 1994 Monte Carlo Modeling in External Electron-Beam Radiotherapy — Why Leave it to Chance? *In "Proceedings of the XI'th Conference on the Use of Computers in Radiotherapy" (Medical Physics Publishing, Madison, Wisconsin)* 2 – 5

Bielajew A F 1995 HOWFAR and HOWNEAR: Geometry Modeling for Monte Carlo Particle Transport *National Research Council of Canada Report PIRS-0341*

Bielajew A F, Hirayama H, Nelson W R and Rogers D W O 1994 History, overview and recent improvements of EGS4 *National Research Council of Canada Report PIRS-0436*

Bielajew A F and Rogers D W O 1987 PRESTA: The Parameter Reduced Electron-Step Transport Algorithm for electron Monte Carlo transport *Nuclear Instruments and Methods* **B18** 165 – 181

Bielajew A F and Rogers D W O 1989 Electron Step-Size Artefacts and PRESTA In T. Jenkins, W. Nelson, A. Rindi, A. Nahum, and D. Rogers (Eds.), *Monte Carlo Transport of Electrons and Photons*, pp. 115 – 137 New York: Plenum Press

Bielajew A F, Rogers D W O and Nahum A E 1985 Monte Carlo simulation of ion chamber response to ^{60}Co – Resolution of anomalies associated with interfaces, *Phys. Med. Biol.* **30** 419 – 428

Bjorken J D and Drell S D 1964 *Relativistic quantum mechanics* International Series in Pure and Applied Physics New York: McGraw-Hill

Bjorken J D and Drell S D 1965 *Relativistic quantum fields* International Series in Pure and Applied Physics New York: McGraw-Hill

Bloch F 1933 Stopping power of atoms with several electrons *Z. für Physik* **81** 363

Bothe W 1921a Das allgemeine Fehlergesetz, die Schwankungen der Feldstärke in einem Dielektrikum und die Zerstreuung der α-Strahlen *Z. für Physik* **5** 63 – 69

Bothe W 1921b Die Gültigkeitsgrenzen des Gaußschen Fehlergesetzes für unabhängige Elementarfehlerquellen *Z. für Physik* **4** 161 – 177

Briesmeister J 1986 MCNP—A general purpose Monte Carlo code for neutron and photon transport, Version 3A *Los Alamos National Laboratory Report LA-7396-M (Los Alamos, NM)*

Briesmeister J F 1993 MCNP—A general Monte Carlo N-particle transport code *Los Alamos National Laboratory Report LA-12625-M (Los Alamos, NM)*

Briesmeister J F 1997 MCNP—A general Monte Carlo N-particle transport code *Los Alamos National Laboratory Report LA-12625-M, Version 4B (Los Alamos, NM)*

Compton A H and Allison S K 1935 X-rays in theory and experiment *(D. Van Nostrand Co. Inc, New York)*

Davies H, Bethe H A and Maximon L C 1954 Theory of bremsstrahlung and pair production. II. Integral cross sections for pair production *Phys. Rev.* **93** 788

de Buffon G C 1777 *Essai d'arithmétique morale*, Volume 4 Supplément à l'Histoire Naturelle

Ehrman J R 1981 The care and feeding of random numbers *SLAC VM Notebook, Module 18, SLAC Computing Services*

Evans R D 1955 *The Atomic Nucleus* New York: McGraw-Hill

Eyges L 1948 Multiple scattering with energy loss *Phys. Rev.* **74** 1534

Feller W 1967 *An introduction to probability theory and its applications, Volume I, 3rd Edition* New York: Wiley

Fernández-Varea J M, Mayol R, Baró J and Salvat F 1993 On the theory and simulation of multiple elastic scattering of electrons *Nuclear Instruments and Methods* **B73** 447 – 473

Goudsmit S A and Saunderson J L 1940a Multiple scattering of electrons *Phys. Rev.* **57** 24 – 29

Goudsmit S A and Saunderson J L 1940b Multiple scattering of electrons. II *Phys. Rev.* **58** 36 – 42

Halbleib J 1989 Structure and Operation of the ITS code system In T. Jenkins, W. Nelson, A. Rindi, A. Nahum, and D. Rogers (Eds.), *Monte Carlo Transport of Electrons and Photons*, pp. 249 – 262 New York: Plenum Press

Halbleib J A, Kensek R P, Mehlhorn T A, Valdez G D, Seltzer S M and Berger M J 1992 ITS Version 3.0: The Integrated TIGER Series of coupled electron/photon Monte Carlo transport codes *Sandia report SAND91-1634*

Halbleib J A and Mehlhorn T A 1984 ITS: The integrated TIGER series of coupled electron/photon Monte Carlo transport codes *Sandia Report SAND84-0573*

Heitler W 1954 The quantum theory of radiation *(Clarendon Press, Oxford)*

Hubbell J H and Øverbø I 1979 Relativistic atomic form factors and photon coherent scattering cross sections *J. Phys. Chem. Ref. Data* **9** 69

James F 1988 A review of pseudorandom number generators *CERN-Data Handling Division, Report DD/88/22*

James F 1994 RANLUX: A FORTRAN implementation of the high-quality pseudorandom number generator of Lüscher *Computer Physics Communications* **79** 111 – 114

Johns H E and Cunningham J R 1983 *The Physics of Radiology, Fourth Edition* Springfield, Illinois: Charles C. Thomas

Kalos M H and Whitlock P A 1986 *Monte Carlo methods, Volume I: Basics* New York: John Wiley and Sons

Kawrakow I and Bielajew A F 1998a On the condensed history technique for electron transport *Nuclear Instruments and Methods* **B142** 253 – 280

Kawrakow I and Bielajew A F 1998b On the representation of electron multiple elastic-scattering distributions for Monte Carlo calculations *Nuclear Instruments and Methods* **B134** 325 – 336

Klein O and Nishina Y 1929 *Z. für Physik* **52** 853

Knuth D E 1981 *Seminumerical algorithms*, Volume II of *The art of computer programming* Reading Mass.: Addison Wesley

Knuth D E 1997 *Seminumerical algorithms*, Volume II of *The art of computer programming* Reading Mass.: Addison Wesley

Koch H W and Motz J W 1959 Bremsstrahlung cross-section formulas and related data *Rev. Mod. Phys.* **31** 920 – 955

Landau L 1944 On the energy loss of fast particles by ionization *J. Phys. USSR* **8** 201

Laplace P S 1886 Theorie analytique des probabilités, Livre 2 In *Oeuvres complétes de Laplace*, Volume 7, Part 2, pp. 365 – 366 Paris: L'académie des Sciences

Larsen E W 1992 A theoretical derivation of the condensed history algorithm *Ann. Nucl. Energy* **19** 701 – 714

Lindeberg J W 1922 Eine neue Herleitung des Exponentialgesetzes in der Wahrscheinlichkeitrechnung *Mathematische Zeitschrift* **15** 211 – 225

Lüscher M 1994 A portable high-quality random number generator for lattice field theory simulations *Computer Physics Communications* **79** 100 – 110

Mackie T R 1990 Applications of the Monte Carlo method in radiotherapy *in Vol. III of "Dosimetry of Ionizing Radiation" eds. K. Kase, B. Bjärngard and F.H. Attix (Academic Press, New York)* 541 – 620

Marsaglia G and Zaman A 1991 A new class of random number generators *Annals of Applied Probability* **1** 462 – 480

Marsaglia G, Zaman A and Tsang W W 1990 Toward a universal random number generator *Statistics and Probability Letters* **8** 35 – 39

Mayol R and Salvat F 1997 Total and transport cross sections for elastic scattering of electrons by atoms *Atomic Data and Nuclear Data Tables* **65** 55–154

Molière G Z 1947 Theorie der Streuung schneller geladener Teilchen. I. Einzelstreuung am abgeschirmten Coulomb-Field *Z. Naturforsch* **2a** 133 – 145

Molière G Z 1948 Theorie der Streuung schneller geladener Teilchen. II. Mehrfach- und Vielfachstreuung *Z. Naturforsch* **3a** 78 – 97

Møller C 1932 *Ann. Phys.* **14** 531

Motz J W, Olsen H A and Koch H W 1969 Pair production by photons *Rev. Mod. Phys.* **41** 581 – 639

Nahum A E 1989 Overview of Photon and Electron Monte Carlo In T. Jenkins, W. Nelson, A. Rindi, A. Nahum, and D. Rogers (Eds.), *Monte Carlo Transport of Electrons and Photons*, pp. 3 – 20 New York: Plenum Press

Nelson W R, Hirayama H and Rogers D W O 1985 The EGS4 Code System Report SLAC–265, Stanford Linear Accelerator Center, Stanford, Calif

Nelson W R and Jenkins T M 1987 Writing subroutine HOWFAR for EGS4 *Stanford Linear Accelerator Center Report SLAC-TN-87-4 (Stanford Calif)*

Olmsted J M H 1947 Solid Analytic Geometry *(Appleton-Century-Crofts Inc, New York)*

Perkins S T, Cullen D E and Seltzer S M 1991 Tables and Graphs of Electron-Interaction Cross Sections from 10 eV to 100 GeV Derived from the LLNL Evaluated Electron Data Library (EEDL), Z = 1–100 *Lawrence Livermore National Laboratory Report UCRL-50400, Volume 31 (Livermore, Calif)*

Rayleigh L 1871 *Phil. Mag.* **XLI** 107

Rogers D W O and Bielajew A F 1990 Monte Carlo techniques of electron and photon transport for radiation dosimetry In K. Kase, B. Bjärngard, and F. Attix (Eds.), *The Dosimetry of Ionizing Radiation, Vol III*, pp. 427 – 539 Academic Press

Sakurai J J 1967 *Advanced quantum mechanics* Reading, Massachusetts: Addison-Wesley

Salvat F, Fernández-Varea J M, Baró J and Sempau J 1996 PENELOPE, an algorithm and computer code for Monte Carlo simulation of electron-photon showers *University of Barcelona Ciemat (Contro de Investigaciones Energéticas, Medioambientales y Tecnolǵicas) Report 799*

Salvat F and Mayol R 1993a Elastic scattering of electrons and positrons by atoms. schrodinger and dirac partial wave analysis *Comput. Phys. Commun.* **74** 358 – 374

Salvat J M F V F and Mayol R 1993b Cross sections for elastic scattering of fast electrons and positron by atoms *Nuclear Instruments and Methods* **B82** 39 – 45

Sauter F 1931 Über den atomaren Photoeffekt in der K-Schale nach der relativistischen Wellenmechanik Diracs *Ann. Physik* **11** 454 – 488

Seltzer S M 1989 An overview of ETRAN Monte Carlo methods In T. Jenkins, W. Nelson, A. Rindi, A. Nahum, and D. Rogers (Eds.), *Monte Carlo Transport of Electrons and Photons*, pp. 153 – 182 New York: Plenum Press

Seltzer S M 1991 Electron-photon Monte Carlo calculations: the ETRAN code *Int'l J of Appl. Radiation and Isotopes* **42** 917 – 941

Sempau J, Acosta E, Baró J, Fernández-Varea J M and Salvat F 1997 An algorithm for Monte Carlo simulation of coupled electron-photon showers *Nuclear Instruments and Methods* **B132** 377 – 390

Shultis J K and Faw R E 1996 *Radiation Shielding* Upper Saddle River: Prentice Hall

Tsai Y S 1974 Pair Production and Bremsstrahlung of Charged Leptons *Rev. Mod. Phys.* **46** 815

Vavilov P V 1957 Ionization losses of high-energy heavy particles *Soviet Physics JETP* **5** 749

Wentzel G 1922 Zur theorie der streuung von β-strahlen *Ann. Physik* **69** 335 – 368